Optimization of Planar Devices by the Finite Element Method

PABLO GARCIA AND J. P. WEBB, MEMBER, IEEE

Abstract —**The finite element method has been shown to be an efficient and flexible way of computing the scattering parameters of N-port planar devices (microstrip. stripline, rectangular waveguide, etc.). In addition, it can provide at little extra cost the sensitivity of scattering parameters to changes in the shape of the device. Such information may be useful in itself; it also leads to a faster automatic optimization of the shape. This approach has been implemented with high-order, triangular finite elements and the Broyden–Fletcher–Goldfarb–Shanno optimization scheme. Sensitivities were computed for an empty parallel-plate waveguide and for a rectangular waveguide containing a dielectric slab: the agreement with analytical solutions was excellent. The method was used to determine the optimum shape of a microstrip 3 dB hybrid and was found to require far fewer analyses than a previous technique [2].**

I. Introduction

A PLANAR DEVICE may be defined as one in which the electromagnetic fields do not vary significantly in one direction, so that the analysis can be carried out in a plane. A junction of rectangular waveguides with their H planes aligned is an example of a perfectly planar device: provided the incident waves are all of the fundamental mode, the fields in the junction will not vary with distance perpendicular to the H plane. By replacing the conducting sidewalls by magnetic walls, a second class of planar devices is obtained: the H-plane junction of parallel-plate waveguides.

In microstrip and stripline components, the fields vary in all three dimensions. However, below the metal plate and away from the edges the variation in the direction perpendicular to the plate is small. Furthermore, the effects of the fringing fields at the edges can be approximated by an extra width of metal, followed by a magnetic wall. This approximation amounts to replacing the microstrip or stripline with equivalent parallel-plate waveguide. Formulas for the dimensions and dielectric constant of the equivalent model have been derived and used in several analyses [1]–[3].

The parallel-plate waveguide junction is therefore of some interest. For the analysis of arbitrary shapes, numerical methods must be used and several have been developed [1], [3]–[5]. Further, there have been some attempts at getting a computer to predict the best shape for a planar device, i.e., predicting the shape that minimizes return loss, gives a specified phase shift or division of power, and so on. The basic approach to automatic optimization is simple: use the numerical analysis method repeatedly, adjusting the shape of the device each time in such a way as to improve the performance. In principle, any reliable method of analysis will do. Integral equation techniques [2] and mode matching [6] have been used.

An important consideration in optimization is efficiency. There are two ways in which the computer time can be reduced: using a more efficient analysis technique and decreasing the number of analyses needed to reach the optimum. In the former regard, the finite element method with appropriate sparse matrix techniques is competitive with other techniques, such as integral equation (or boundary element) methods. But further, it is shown in this paper how the finite element method can provide, at little extra cost, the sensitivity of the scattering parameters to changes in shape. Not only might this information be useful in itself, but, as described below, it can be used to guide the optimization of the device and to reduce substantially the number of analyses required.

Manuscript received March 23, 1989; revised July 25, 1989. This work was supported by the Natural Sciences and Engineering Research Council of Canada and the Centre de Recherche Informatique de Montréal.

P. Garcia was with the Department of Electrical Engineering, McGill University, Montréal, Québec, Canada H3A 2A7. He is now with MPB Technologies, Montréal, Québec, Canada.

J. P. Webb is with the Computational Analysis and Design Laboratory, Department of Electrical Engineering, McGill University, 3480 University Street, Montréal, Québec, Canada H3A 2A7.

IEEE Log Number 8931559.

II. Finite Element Analysis of Planar Devices

The scalar Helmoltz equation governs E, the y component of the electric field in a planar device:

$$\nabla_t^2 E + k_0^2 \epsilon_r E = 0 \qquad \text{in } \Omega \tag{1}$$

$$E = E_0 \qquad \text{on } \partial\Omega_D$$

$$\frac{\partial E}{\partial n} = 0 \qquad \text{on } \partial\Omega_N$$

$$\nabla_t = \boldsymbol{a}_z \frac{\partial}{\partial z} + \boldsymbol{a}_x \frac{\partial}{\partial x}$$

where Ω is the area of the device in the $z-x$ plane, ϵ_r is the relative permittivity of the medium, k_0 is the normalized frequency, and E_0 is the prescribed tangential field at the port. The quantity $\partial\Omega_N$ is a magnetic wall or open circuit (O/C). When E_0 is zero, $\partial\Omega_D$ is an electric wall or short circuit (S/C).

0018-9480/90/0100-0048$01.00

Alternatively, it has been shown [7] that the solution to the above equation is the stationary point of a functional:

$$F(E)=\frac{1}{2}\int_{\Omega}\left\{(\nabla_t E)^2-k_0^2\epsilon_r E^2\right\}d\Omega. \qquad (2)$$

This is the basis of the finite element analysis of planar devices [8]. By introducing trial functions, (2) is reduced to a matrix form:

$$F=\frac{1}{2}[E]^T([S]-k_0^2[T])[E] \qquad (3)$$

where $[S]$ and $[T]$ are well-known global matrices [7]. Taking the stationary point of F and applying boundary conditions leads to a matrix equation of the form $[A][E]=[b]$, in which $[A]$ is sparse and symmetric. It is important to solve this equation with a method that exploits the sparsity. In the present work, a frontal solver is used [9].

It is convenient to characterize a planar device by network parameters. A variational expression exists for the impedance matrix of a waveguide junction [10]. Using this result, the finite element method was used to solve 3-D waveguide problems [11]. It was shown that for H-plane devices [8] the entries of the admittance matrix are given by an expression similar to (2):

$$[Y]_{mn}=\frac{-jb}{k_0\eta_0}\langle E^{(m)},E^{(n)}\rangle \qquad (4)$$

where

$$\langle\phi,\psi\rangle=\int_{\Omega}\left\{\nabla_t\phi\cdot\nabla_t\psi-k_0^2\epsilon_r\phi\psi\right\}d\Omega \qquad (5)$$

and

$m, n=1,\cdots,N$

- N number of ports,
- η_0 intrinsic impedance of free space,
- b dimension of the structure in the direction of translational symmetry,
- $[Y]$ normalized admittance matrix for the device, defined by $[I]=[Y][V]$, where $[I]$ and $[V]$ are column vectors of normalized currents and voltages [12] at the ports,
- $E^{(k)}$ electric field when there is a normalized voltage of 1 on port k and all other ports are short-circuited.

$E^{(k)}$ is obtained by taking the first variation of (2) when exciting port k and short-circuiting all other ports. The entries of the admittance matrix are obtained by matrix multiplication of the solution vectors $[E^{(k)}]$ with the global matrices:

$$[Y]_{mn}=\frac{-jb}{k_0\eta_0}[E^{(m)}]^T\{[S]-k_0^2[T]\}[E^{(n)}]. \qquad (6)$$

The scattering matrix is then given by

$$[S]=([I_0]+[Y])^{-1}([I_0]-[Y]) \qquad (7)$$

where $[I_0]$ is the $N\times N$ identity matrix.

III. Sensitivity to Perturbations

Finite elements have been used in the past to evaluate the sensitivity of magnetostatic energy to perturbations of shape, both for optimization [13] and for the calculation of forces and torques by the principle of virtual work [14]. In this paper it will be shown how the sensitivity of network parameters to perturbations of shape can be obtained from a finite element analysis.

A. Derivative with Respect to an Arbitrary Geometric Parameter

Let the shape of the region Ω_g be dependent on a scalar parameter g in the following way: each point $\boldsymbol{r}_g$ in Ω_g is related to a point $\boldsymbol{r}$ in a reference region Ω by

$$\boldsymbol{r}_g=\boldsymbol{r}+g\boldsymbol{v} \qquad (8)$$

where $\boldsymbol{v}$ is a specified vector function over Ω. Let $E_g^{(m)}$ be the solution to the Helmoltz equation over the region Ω_g, with port m excited and the other ports shorted. Define a symmetric, bilinear form $\langle\phi,\psi\rangle$ as follows:

$$\langle\phi,\psi\rangle_g=\int_{\Omega_g}\left\{\nabla_t\phi\cdot\nabla_t\psi-k_0^2\epsilon_r\phi\psi\right\}d\Omega_g. \qquad (9)$$

From (4) the mnth entry of the admittance matrix $[Y](g)$ is

$$[Y]_{mn}(g)=\frac{-jb}{k_0\eta_0}\langle E_g^{(m)},E_g^{(n)}\rangle_g. \qquad (10)$$

Then it can be shown [15] that the derivative of the admittance with respect to g, evaluated at $g=0$, is

$$\left.\frac{d[Y]_{mn}}{dg}\right|_{g=0}=\frac{-jb}{k_0\eta_0}(E^{(m)},E^{(n)}) \qquad (11)$$

where (ϕ,ψ) is another symmetric, bilinear form:

$$(\phi,\psi)=\int_{\Omega}\left\{\nabla_t\cdot\boldsymbol{v}\nabla_t\phi\cdot\nabla_t\psi-\sum_{i=1}^{i=2}\sum_{j=1}^{j=2}\frac{\partial v_j}{\partial r_i}\left[\frac{\partial\phi}{\partial r_i}\frac{\partial\psi}{\partial r_j}+\frac{\partial\phi}{\partial r_j}\frac{\partial\psi}{\partial r_i}\right]-k_0^2\epsilon_r\phi\psi\nabla_t\cdot\boldsymbol{v}\right\}d\Omega \qquad (12)$$

and $(r_1,r_2)=(z,x)$.

B. Derivative with Respect to a Single Vertex Coordinate in a Finite Element Mesh

In the finite element method, the region Ω is divided into triangles. The geometry of the region is then dependent on the coordinates of the vertices of these triangles. In this section, we evaluate (11) for a deformation of Ω corresponding to the movement of a single vertex along one coordinate axis, with all other vertices remaining fixed.

If the moving vertex has a global number k, and the movement is along axis r_l (l being 1 or 2), then we need a $\boldsymbol{v}$ such that

$$\boldsymbol{v}(\boldsymbol{r})=\begin{cases}\boldsymbol{a}_l & \text{at } \boldsymbol{r}=\boldsymbol{r}^{(k)}\\ 0 & \text{at } \boldsymbol{r}=\boldsymbol{r}^{(i)},\ i\neq k\end{cases} \qquad (13)$$

where $\boldsymbol{a}_l$ is the unit vector in the r_l direction, and $\boldsymbol{r}^{(k)}$ is the position vector of vertex k.

Such a $\boldsymbol{v}$ can be constructed by linear interpolation of the vertex values; i.e., $\boldsymbol{v}$ is a continuous, first-order vector field on each triangle. Let $\bar{k}$ be the local vertex number (1, 2, or 3) of node k in element h. Then in that element,

$$\boldsymbol{v} = \zeta_{\bar{k}} \boldsymbol{a}_l \tag{14}$$

where $\zeta_{\bar{k}}$ is the $\bar{k}$th area coordinate [7]. The derivative $d[Y]_{mn}/dg$ at $g=0$ for this $\boldsymbol{v}$ will be called

$$\frac{d[Y]_{mn}}{dr_l^{(k)}}.$$

Also in element h,

$$E_h^{(m)} = \sum_{i=1}^{i=n_0} E_{hi}^{(m)} \alpha_i(\zeta_1, \zeta_2, \zeta_3)$$

$$n_0 = \frac{(n+1)(n+2)}{2} \tag{15}$$

where $\alpha_1, \alpha_2, \cdots, \alpha_{n_0}$ are the Lagrange interpolation polynomials used in nth-order triangular elements [7], and $[E_h^{(m)}]$ is a column vector containing the values of the y-directed electric field at the n_0 nodes of the element. Now from (11) and (14),

$$\frac{d[Y]_{mn}}{dr_l^{(k)}} = \frac{-jb}{k_0 \eta_0} \sum_h \left(E_h^{(m)}, E_h^{(n)}\right)_l^{(\bar{k}h)} \tag{16}$$

where

$$(\phi, \psi)_l^{(\bar{k}h)} = \int_{\Delta_h} \left\{ \frac{\partial \zeta_{\bar{k}}}{\partial r_l} \nabla_t \phi \cdot \nabla_t \psi - \sum_{i=1}^{i=2} \sum_{j=1}^{j=2} \frac{\partial \zeta_{\bar{k}}}{\partial r_i} \delta_{lj} \left[\frac{\partial \phi}{\partial r_i} \frac{\partial \psi}{\partial r_j} + \frac{\partial \phi}{\partial r_j} \frac{\partial \psi}{\partial r_i} \right] - k_0^2 \epsilon_r \phi \psi \frac{\partial \zeta_{\bar{k}}}{\partial r_l} \right\} d\Omega \tag{17}$$

and the summation is over all triangles sharing node k. Substituting (15) into (17) and assuming ϵ_r to be constant in each triangle gives, after some algebra,

$$\left(E_h^{(m)}, E_h^{(n)}\right)_l^{(\bar{k}h)} = \left[E_h^{(m)}\right]^T \left\{ \left[S_l^{(\bar{k}h)}\right] - k_0^2 \left[T_l^{(\bar{k}h)}\right] \right\} \left[E_h^{(n)}\right] \tag{18}$$

where

$$\left[S_l^{(\bar{k}h)}\right] = \sum_{p=1}^{p=3} \sum_{q=1}^{q=3} \sum_{i=1}^{i=2} \left[d_{pi} d_{\bar{k}l} d_{qi} - d_{\bar{k}i} \left(d_{pi} d_{ql} + d_{pl} d_{qi} \right) \right] \cdot \left[K^{(pq)}\right] \tag{19}$$

$$\left[T_l^{(\bar{k}h)}\right] = \epsilon_r d_{\bar{k}l} [T] \tag{20}$$

$$d_{j1} = x^{j+1} - x^{j-1} \tag{21}$$

$$d_{j2} = z^{j-1} - z^{j+1} \tag{22}$$

with $(z^{(j)}, x^{(j)})$ the coordinates of vertex j of triangle h. In the latter two expressions the superscripts are cyclic; i.e., if $j=3$, $j+1=1$. $[K^{pq)}]$ and $[T]$ are n_0 by n_0 universal matrices [16].

C. Derivative with Respect to a Combined Movement of Vertices in a Finite Element Mesh

The derivatives with respect to vertex coordinates shown above may be related to other geometric parameters that describe the optimization problem. Let a set of geometric parameters g_j ($j=1,2,\cdots,N_g$) specify a movable boundary $\partial\Omega_m$ in the following way: Let $(r_1^{(i)}, r_2^{(i)})$, $i=1,2,\cdots,m_0$, be m_0 triangle vertices lying on $\partial\Omega_m$. For $i=1,2,\cdots,m_0$ and $l=1,2$,

$$r_l^{(i)} = \sum_{j=1}^{j=N_g} [R_l]_{ij} g_j + [c_l]_{ij} \tag{23}$$

where $[R_l]_{ij}, [c_l]_{ij}$ are constant, user-specified coefficients. This leads to the simple relation for a gradient with respect to the geometric parameters:

$$\nabla_g [Y]_{mn} = \sum_{l=1}^{l=2} [R_l]^T \nabla_{r_l} [Y]_{mn} \tag{24}$$

where

$$\nabla_g [Y]_{mn} = \begin{bmatrix} \frac{\partial [Y]_{mn}}{\partial g_1} \\ \vdots \\ \frac{\partial [Y]_{mn}}{\partial g_{N_g}} \end{bmatrix}$$

and

$$\nabla_{r_l} [Y]_{mn} = \begin{bmatrix} \frac{\partial [Y]_{mn}}{\partial r_l^{(1)}} \\ \vdots \\ \frac{\partial [Y]_{mn}}{\partial r_l^{(m_0)}} \end{bmatrix}.$$

From the above result and (7) the sensitivity of scattering parameters to geometric variation is readily available:

$$\nabla_g [S] = -([I_0] + [Y])^{-1} \nabla_g [Y] ([S] + [I_0]). \tag{25}$$

IV. Optimization

The quality of a design can be assessed by a cost function, a single figure of merit which an automatic optimizer tries to reduce to a minimum.

For example, to minimize return loss at one frequency for a 1-port network, a suitable cost function would be simply $C = |S_{11}|^2$. A more complicated cost function for a 4-port device is given in Section V, below. As long as the cost function C can be expressed in terms of the scattering parameters $[S]$, the derivatives $\nabla_g C$ can be evaluated from a knowledge of $\nabla_g [S]$ (25).

To take full advantage of the availability of $\nabla_g C$, we have used a quasi-Newton optimization method [17]. The geometric parameters are updated as follows:

$$\left[g^{(k+1)}\right] = \left[g^{(k)}\right] + v^{(k)} \left[p^{(k)}\right] \tag{26}$$

where $v^{(k)}$ is the step size in the search direction $[p^{(k)}]$ in

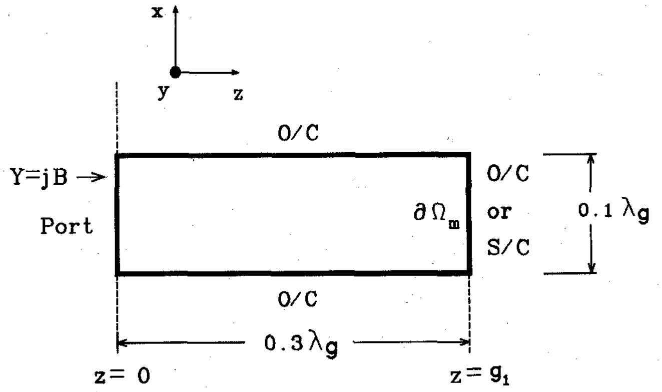

Fig. 1. Uniform air-filled parallel-plate waveguide. The open circuit (O/C) and short circuit (S/C) correspond to a magnetic wall and conductor boundary respectively.

an N_g-dimensional space. The value of $v^{(k)}$ is found in a line search which makes use of $\nabla_g C$ and combines cubic interpolation with quadratic polynomial extrapolation [17]. The search direction $[p^{(k)}] = -[H^{(k)}]\nabla_g C^{(k)}$ is generated by updating an approximate inverse-Hessian $[H^{(k)}]$ using the BFGS (Broyden–Fletcher–Goldfarb–Shanno) method. As the geometric parameters change at each iteration Δg_j in (26), the coordinates of the vertices lying on the boundary $\partial\Omega_m$ will change as follows (from (23)):

$$\Delta r_l^{(i)} = \sum_{j=1}^{j=N_g} [R_l]_{ij} \Delta g_j. \tag{27}$$

Following each change of the vertex coordinates, the entire region is automatically remeshed using Delauney triangulation [18]. The remeshing was found to be inexpensive compared to the analysis of the problem.

V. Results

A computer program package SOFIE (Scattering-Parameter Optimization by FInite Elements) has been written in Fortran-77 to implement the theory described above for the design of planar devices [15]. Three examples were selected with a twofold purpose: to verify the accuracy of $\nabla_g[Y]$ and $\nabla_g[S]$ and to validate the software implementation for design and optimization. All the results in this section were obtained on a DEC Microvax II running Ultrix V1.2.

A. Parallel-Plate Waveguide

A uniform, air-filled parallel-plate waveguide carrying the dominant mode (TEM) with $\beta = k_0 = 2\pi$ is shown in Fig. 1. The guide wavelength is λ_g. Let g_1 be a geometric parameter defining the distance of $\partial\Omega_m$ from the port. The object was to compute the normalized susceptance B at the port, and the corresponding derivative with respect to g_1, for two types of boundary conditions on $\partial\Omega_m$: open circuit and short circuit. The analytical solutions can be obtained in closed form from transmission line theory [12].

The problem was discretized with 14 elements and 13 vertices. The results obtained from finite element analysis are compared with the analytical values (in parentheses) in Table I. There is excellent agreement with the analytical results with increasing order of polynomial trial functions.

TABLE I
Results for the Empty Parallel-Plate Waveguide

Polynomial Order	OPEN CIRCUIT		SHORT CIRCUIT	
	Error (%) B (-3.07768)	Error (%) $\frac{dB}{dg_1}$ (65.7984)	Error (%) B (0.324920)	Error (%) $\frac{dB}{dg_1}$ (6.94652)
1	+5.89	+6.72	-8.10	+3.90
2	+0.06	+0.04	+0.31	-0.05
3	+0.03	-0.01	+0.03	-0.01
4	+0.00	+0.00	+0.01	+0.01

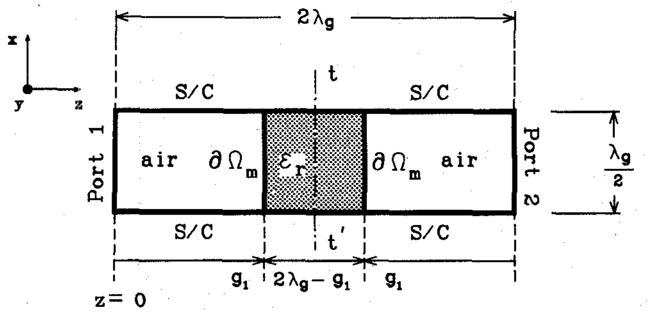

Fig. 2. Rectangular waveguide filled with a slab of dielectric of relative permittivity $\epsilon_r = 1.5$.

B. Rectangular Waveguide with Dielectric Slab

A uniform rectangular waveguide filled with a slab of dielectric and carrying the dominant mode TE_{10} is shown in Fig. 2. λ_g is the guide wavelength in the air region where the propagation constant is $\beta_1 = \pi/2$ rad m^{-1}. The dielectric region has a propagation constant $\beta_2 = \pi/\sqrt{2}$ rad m^{-1} and relative permittivity $\epsilon_r = 1.5$. In this case the geometric parameter g_1 is the length of the air-filled section on either side of the slab. This example possesses a plane symmetry about tt'; therefore only half of the problem was modeled [19]. As g_1 varies the electrical length of the waveguide changes, so $\angle S_{21}$ changes. The analytical solutions were obtained from transmission line theory [12].

The problem was analyzed with about 90 elements and 60 vertices. A graph of $d\angle S_{21}/dg_1$ versus g_1 is plotted from the results for second- and fourth-order elements in Fig. 3. The graph shows that close agreement exists with the analytical values for a wide range of g_1.

C. Stripline 3 dB Hybrid Ring

A stripline 3 dB hybrid ring is a directional coupler with a circular outer periphery. This type of device is a 4-port network for which ideally there is no return loss, equal power coupling at two ports, and a matched fourth port;

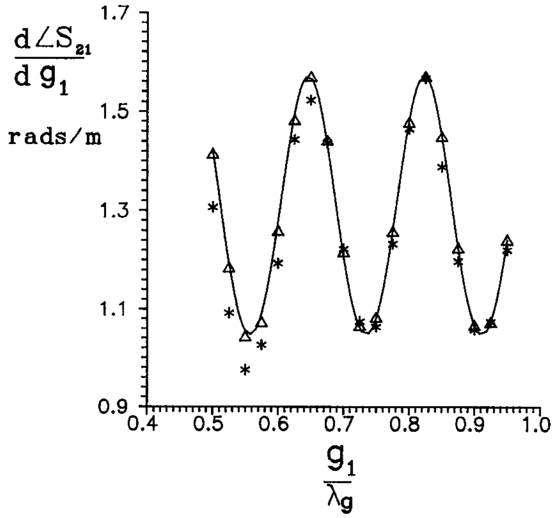

Fig. 3. Analytical (curve) and finite element (points) results for the derivative $d\angle S_{21}/dg_1$. Asterisks and triangles correspond to second- and fourth-order elements respectively.

i.e., the ideal scattering matrix $[\bar{S}]$ has the properties

$$|\bar{S}_{11}|^2 = |\bar{S}_{41}|^2 = 0 \qquad |\bar{S}_{21}|^2 = |\bar{S}_{31}|^2 = 0.5. \quad (28)$$

The model considered is based on an earlier example [2]. The incoming stripline has a characteristic impedance of 50 Ω; there is an even spacing of 1.45 mm between middle conductor and the ground plates; the dielectric material has relative permittivity $\epsilon_r = 2.53$; and the center frequency is $f_0 = 4.94$ GHz. The device possesses double symmetry and so only one quarter of it was analyzed with different permutations of open (O/C) and short circuits (S/C) [19].

The characteristics in (28) are required to hold symmetrically over a frequency range $(0.9f_0, 1.1f_0)$. The cost function C minimized was the same as that used in [2]:

$$C = F_1 + F_2 \quad (29)$$

$$F_1 = \sum_{i=1}^{i=4} \left\{ \left[|S_{i1}(0.9f_0)|^2 - |\bar{S}_{i1}|^2 \right]^2 + 10\left[|S_{i1}(f_0)|^2 - |\bar{S}_{i1}|^2 \right]^2 + \left[|S_{i1}(1.1f_0)|^2 - |\bar{S}_{i1}|^2 \right]^2 \right\} \quad (30)$$

$$F_2 = \sum_{i=1}^{i=4} 2\left[|S_{i1}(1.1f_0)|^2 - |S_{i1}(0.9f_0)|^2 \right]^2. \quad (31)$$

The geometric parameters g_i $(i = 1,2,3,\cdots,N_g)$ with $N_g = 17$ were assigned along a circular inner periphery $\partial\Omega_m$ (see Fig. 4). Each parameter g_i is the distance of one of 17 equally spaced vertices from the origin. The initial shape is $g_i^{(0)} = 5.0$ mm for $i = 1,2,3,\cdots,N_g$, and the coefficients $[R_l]_{ji}$ for the vertices on the boundary $\partial\Omega_m$ are given by

$$[R_1]_{ji} = \cos\theta_j \delta_{ij} \qquad [R_2]_{ji} = \sin\theta_j \delta_{ij}.$$

In addition, the coefficients $[R_l]_{ji}$ were doubled for the two vertices that lay on planes of symmetry, because this was found to keep the boundary smooth during the optimization.

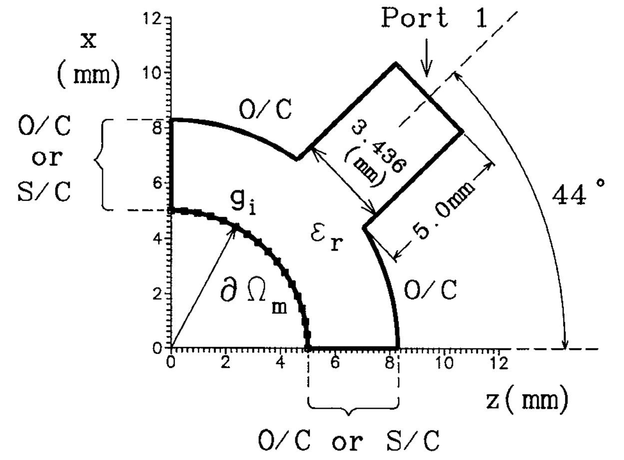

Fig. 4. Initial shape of one quarter of the model for a hybrid ring.

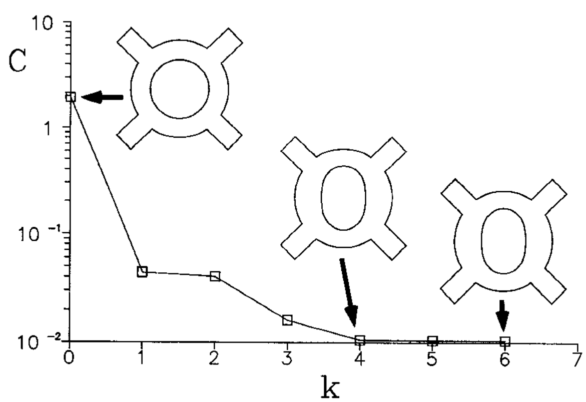

Fig. 5. Cost function versus search directions k in an N_g-dimensional space.

TABLE II
COMPARISON OF THE OPTIMIZATION PROCESS OF THE HYBRID RING WITH AN EARLIER METHOD

Case	Method of Optimization	Cost Function (Start)	Cost Function (End)	Degrees of Freedom	Number of Line Searches	Function Evaluations (Analyses)
[2]	Powell Method	0.05	0.011	9	52	> 104
SOFIE	BFGS	1.94	0.010	17	6	15

The optimization process took 3.5 hours of CPU time. Initially the mesh contained 251 vertices and 428 second-order elements. In Fig. 5 the cost function is compared after each search direction k in a 17-dimensional space. The function was reduced by a factor of 44 after the first search direction $k = 0$. The reduction of the cost function between $k = 4$ and $k = 6$ was less than 0.1 percent with practically no change in the shape of the model.

The results of the optimization are compared with those of a previous method [2] in Table II. The method employed in this paper required far fewer cost function evaluations (analyses). In addition, the starting point in our optimization had a higher cost function; the overall reduction in the cost function was by a factor of 194, compared with 5 in [2].

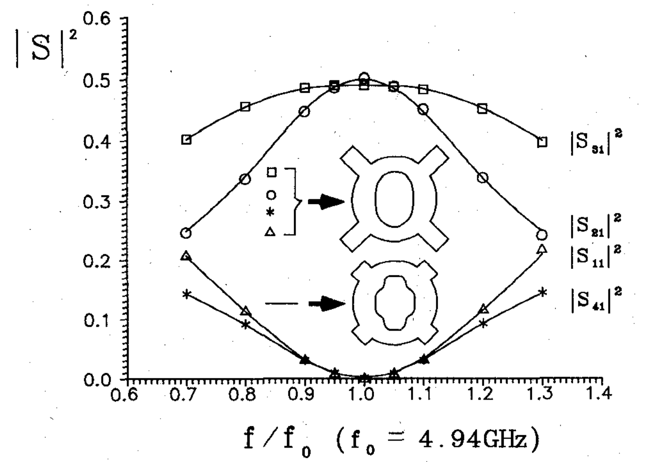

Fig. 6. Frequency response for optimal shapes analyzed by SOFIE. The curves and the points correspond to the shape given in [2] and to that obtained by SOFIE, respectively.

The final optimum shape in this paper is different from that obtained in [2], indicating that there may not be a unique solution to the problem. The scattering characteristics of our optimum are compared with those of [2] in Fig. 6 using the finite element method with third-order elements. The agreement is excellent. External matching circuits could be added on each arm of the hybrid to further improve its frequency response.

VI. Conclusions

When sensitivity information is available, a design can be much improved in just a few successive analyses because the direction in which to change the shape is known. However, this information can usually only be obtained by numerical differentiation, which requires at least $N+1$ analyses if there are N geometric parameters. This adds greatly to the cost of optimization. The finite element method is able to provide sensitivities at almost no cost, thereby providing cheaper optimization.

References

[1] Z. J. Cendes and J. F. Lee, "The transfinite element method for modeling MMIC devices," *IEEE Trans. Microwave Theory Tech.*, vol. 36, pp. 1639–1649, Dec. 1988.

[2] T. Okoshi, T. Imai, and K. Ito, "Computer-oriented synthesis of optimum circuit pattern of 3-dB hybrid ring by the planar circuit approach," *IEEE Trans. Microwave Theory Tech.*, vol. MTT-29, pp. 194–202, Mar. 1981.

[3] K. C. Gupta, R. Garg, and I. J. Bahl, *Microstrip Lines and Slotlines.* Norwood, MA: Artech House, 1979.

[4] T. Okoshi, *Planar Circuits For Microwaves and Lightwaves.* New York: Springer-Verlag, 1984.

[5] P. Arcioni, M. Bressan, and G. Conciauro, "A new algorithm for the wide-band analysis of arbitrarily shaped planar circuits," *IEEE Trans. Microwave Theory Tech.*, vol. 36, pp. 1426–1437, Oct. 1988.

[6] J. Dittloff, F. Arndt, and D. Grauerholz, "Optimum design of waveguide *E*-plane stub-loaded phase shifters," *IEEE Trans. Microwave Theory Tech.*, vol. 36, pp. 582–587, Mar. 1988.

[7] P. P. Silvester and R. L. Ferrari, *Finite Elements For Electrical Engineers.* Cambridge University Press, 1983.

[8] J. P. Webb and S. Parihar, "Finite element analysis of the *H*-plane rectangular waveguide problems," *Proc. Inst. Elec. Eng.*, vol. 133, pt. H, pp. 103–109, Jan. 1986.

[9] B. M. Irons, "A frontal solution program for finite element analysis," *Int. J. Numer. Meth. Eng.*, vol. 15, no. 4, pp. 519–536, 1980.

[10] K. Morishita and K. Nobuaki, "Unified approach to the derivation of variational expression for electromagnetic fields," *IEEE Trans. Microwave Theory Tech.*, vol. MTT-25, pp. 34–40, Jan. 1977.

[11] J. P. Webb, G. L. Maile, and R. L. Ferrari, "Finite-element solution of three-dimensional electromagnetic problems," *Proc. Inst. Elec. Eng.*, vol. 130, pp. 153–159, Mar. 1983.

[12] R. E. Collin, *Foundations for Microwave Engineering.* New York: McGraw-Hill, 1966, p. 147.

[13] A. Marrocco and O. Pironneau, "Optimum design with Lagrangian finite elements: Design of an electromagnet," *Comp. Meth. Appl. Mech. Eng.*, vol. 15, pp. 277–308, 1978.

[14] J. L. Coulomb, G. Meunier, and J. C. Sabonnadiere, "Energy methods for the evaluation of global quantities and integral parameters in a finite elements analysis of electromagnetic devices," *IEEE Trans. Magn.*, vol. MAG-21, pp. 1817–1822, Sept. 1985.

[15] P. Garcia, "Optimization of *H*-plane junctions using finite elements," M. Eng. thesis, McGill University, Canada, Jan. 1989.

[16] P. Silvester, "Construction of triangular finite element matrices", *Int. J. Numer. Meth. Eng.*, vol. 12, pp. 237–244, 1978.

[17] L. E. Scales, *Introduction to Non-linear Optimization.* New York: Springer-Verlag, 1985.

[18] C. F. Bryant, "Two dimensional automatic triangular mesh generation," *IEEE Trans. Magn.*, vol. MAG-21, pp. 2547–2550, Nov. 1985.

[19] J. Helszajn, *Passive and Active Microwave Circuits.* New York: Wiley, 1978.

✠

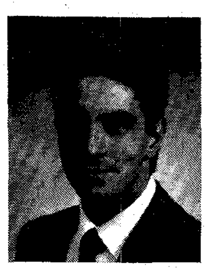

Pablo Garcia was born in Cuenca, Spain, in 1962. He received the B.Sc. Honours in physics degree from Concordia University, Montreal, Canada, in November 1985 and the M.Eng. degree in electrical engineering from McGill University, Montreal, Canada, in June 1989.

In May 1989, he joined MPB Technologies in Montreal and is presently involved in the study of radiation hazards from antennas. His areas of interest are numerical methods in electromagnetics and antenna design and measurement techniques.

✠

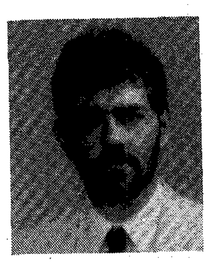

J. P. Webb (M'83) received the Ph.D. degree from Cambridge University, England, in 1981.

Since 1982 he has been an Assistant Professor, then an Associate Professor, in the Electrical Engineering Department of McGill University, Montreal, Canada, His area of research is computer methods in electromagnetics, especially the application of the finite element method.